Front. Earth Sci. 2024, 18(4): 732–742
https://doi.org/10.1007/s11707-024-1120-3

RESEARCH ARTICLE

Evaluation of the effectiveness of shale bedding fractures: a case study of the Longmaxi Formation in the Sichuan Basin

Tao WANG[1], Ziwei LIU[2], Zhiliang HE[3], Hu WANG (✉)[4,5,6], Haijao FU[4,5], Haikuan NIE[3]

1 Chinese Academy of Geological Sciences, Beijing 100037, China
2 China National Petroleum Corp Bureau of Geophysical Prospecting Inc., Tianjin 300280, China
3 Sinopec Petroleum Exploration and Development Research Institute, Beijing 100083, China
4 Key Laboratory of Tectonics and Petroleum Resources, (Ministry of Education), China University of Geosciences, Wuhan 430074, China
5 China University of Geosciences, Wuhan 430074, China
6 Dataskin Technology (Hubei) Co., Ltd., Wuhan 430074, China

Abstract Bedding fractures are among the key factors affecting the production efficiency of shale oil and gas, but relatively little research has been conducted on the effectiveness of bedding fractures. Based on field outcrops and drill cores from the Fuling area in the Sichuan Basin, this work discusses the development, filling, and opening characteristics of bedding fractures and their quantitative impact on physical properties. Multiple methods were employed, e.g., immersion testing, wet illumination, high-power microscanning, imaging logging identification and experimental measurement. The results indicate that the highest density reaches 437 fractures per meter, with apertures less than 0.5 μm being the majority. The average permeability of the shale samples with vertical bedding is 44.6 times that of the shale samples with parallel bedding, while the porosity exhibits less anisotropy. Many open bedding fractures with gas outlets in the core are shown by on-site immersion experiments and electron microscopy scanning experiments. Each dark stripe on the imaging logging map corresponds to a bedding fracture, and the thickness of the dark stripes corresponds to the aperture of the bedding fracture. There is no need to consider unfilled bedding fractures, as fractures filled with calcite veins and pyrite crystals can also become effective seepage channels because of the pores within the calcite veins and between the pyrite crystals. The utilization and transformation of bedding fractures during fracturing is one of the key steps in producing shale oil and gas. It is necessary to combine the *in situ* stress field, bedding fracture characteristics, and fracturability of shales to reasonably utilize bedding fractures to transform oil and gas reservoirs.

Received October 7, 2023; accepted February 2, 2024

E-mail: wanghu19@cug.edu.cn

Keywords bedding fractures, complex fracture network, formation of bedding, Fuling area

1 Introduction

As the world economy has developed, the consumption of oil and gas as primary energy sources has continued to increase, reaching 143.66 × 10^{12} m^3 of oil equivalent in 2022 (BP, 2022). Multiple economic research institutions have predicted that the proportion of oil and gas resources in primary energy consumption will still remain greater than 50% until 2040 (EIA, 2018; Solarin et al., 2020). The important position of oil and gas resources in primary energy is attributed to the large-scale development of shale oil and gas. The shale oil and gas revolution in the United States basically achieved self-sufficiency in oil and gas production and completed the transformation of the United States from an importing country to an exporting country in terms of natural gas (OPEC, 2018; Zou et al., 2020).

Global shale gas resources are abundant and are mainly distributed in North America, Central Asia, China, the Middle East, North Africa, and Southern Africa (Zhou et al., 2012; Zou et al., 2023). At present, the United States has successfully discovered and achieved industrial exploitation of 12 shale oil and gas zones. Shale gas zones in the US mainly include the Eagle Ford, Marcellus, Barnet, Permian Basin, Eutica, Heinsville, and Naibulus (Zou et al., 2023). Shale gas resources in China are mainly distributed in the Songliao Basin, Qiangtang Basin, Tuha Basin, Jungar Basin, Sichuan Basin, and Ordos Basin. The Sichuan Basin and Tarim Basin account for the largest proportion of the total resources, namely, nearly 80% (Dai et al., 2021).

Bedding fractures in shale reservoirs are important factors affecting shale gas development (Wang et al., 2016, 2018b; Sun and Bao, 2018; Liu et al., 2021). Previous researchers have expended much effort determining the causes and effects of bedding fracturing. The formation of bedding fractures is related to sedimentation, tectonic movements, and the evolutionary processes of organic matter. Sedimentary processes and environments are the foundation of bedding fracture formation, and the nonuniformity of the stress field caused by tectonic movements is the external cause of bedding fracture formation (Gale et al., 2014; He et al., 2017a; Wang et al., 2018b, 2021; Liu et al., 2022). The evolution of organic matter generates oil and gas, which increases the fluid pressure in the fracture space and promotes the opening of bedding fractures. The distributions of bedding fractures, organic matter, and brittle minerals are strongly correlated, and their intensity of development and longitudinal stress differences directly affect the scale and complexity of fracture development in reservoirs after fracturing (Zou et al., 2020; Wang et al., 2021). In general, the more the bedding fractures develop, the smaller the height of the developing fractures. However, fracture development increases the spatial complexity of hydraulic fractures, which is beneficial for improving single-well production and the ultimate recovery rate (Li et al., 2021).

Most studies on bedding fractures involve qualitative descriptions of the impact of bedding fractures on geological and engineering scenarios. Relatively little research has attempted to evaluate the reasons for and extent of bedding fracture impacts; therefore, quantitative analysis of bedding fracture effects is necessary. This article aims to analyze the filling and opening characteristics and quantitative effects on the physical properties of shale bedding fractures by drill cores and outcrops utilizing methods such as immersion testing, quantitative analysis of rock cores, scanning electron microscopy, logging evaluation, and indoor physical property analysis experiments. This approach further explores the quantitative impact of bedding fractures on geomechanics at the reservoir scale and thus more efficiently utilizes bedding fractures for shale oil and gas development.

2 Geological background and methods

2.1 Geological background

The Jiaoshiba anticline zone features a box-shaped structure in profile, with an overall flat and wide pattern. Its central part is weakly deformed, the degree of fracture development is low (Fig. 1), and the dip angle of the strata is less than 5°. The degree of deformation of the Jiaoshiba anticline limbs is relatively high, and the degree of development of fractures is also high, with an average formation dip angle greater than 5° (He et al., 2017a).

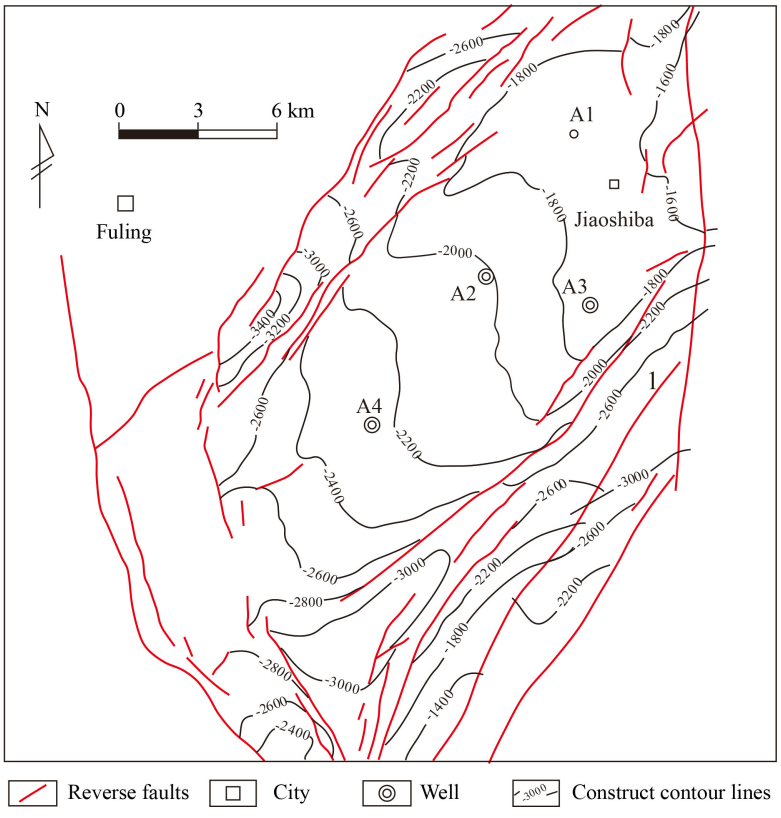

Fig. 1 Structural map of the study area.

The major faults in the Fuling gas field generally strike north-east, but the northern fault of Jiaoshiba clearly shows a leftward deviation, and the internal Wujiang Fault and the north-west small fault to the west of the Diaoshuiyan Fault formed in the later stage. Previous works showed that the north-east-trending structure in the study area formed during the early stage and was later compressed by the north-west-trending structure to form a north-west-trending fault, which transformed the existing north-east-trending fault. Consequently, fault patterns have formed in the current target research area (Guo et al., 2017; Wang et al., 2019c; Zhao et al., 2023). The research area features two main sets of faults, north-east- and north-west-oriented, which formed in the late stage of the Yanshan Movement and were the result of east–west compressive stress generated by the subduction of the Pacific Plate (He et al., 2019). Core and layer samples were collected mainly from the bottom section of the Upper Ordovician Wufeng Formation and Lower Silurian Longmaxi Formation in the Guanyinqiao, Pengshui Lujiao, and Shizhu Qiliao sections of Qijiang, Chongqing, as well as from the A1, A2, and A3 wells of the Jiaoshiba shale gas field.

The drilling data from the JY1 well show that the strata in the study area lack the Devonian system, whereas the Carboniferous system contains only the Huanglong Formation. The other formations are relatively well integrated (Fig. 2(a)). The target layers in the study area are the Wufeng and Longmaxi shales (Fig. 2(b)) (Nie et al., 2021). The total thicknesses of high-quality shale

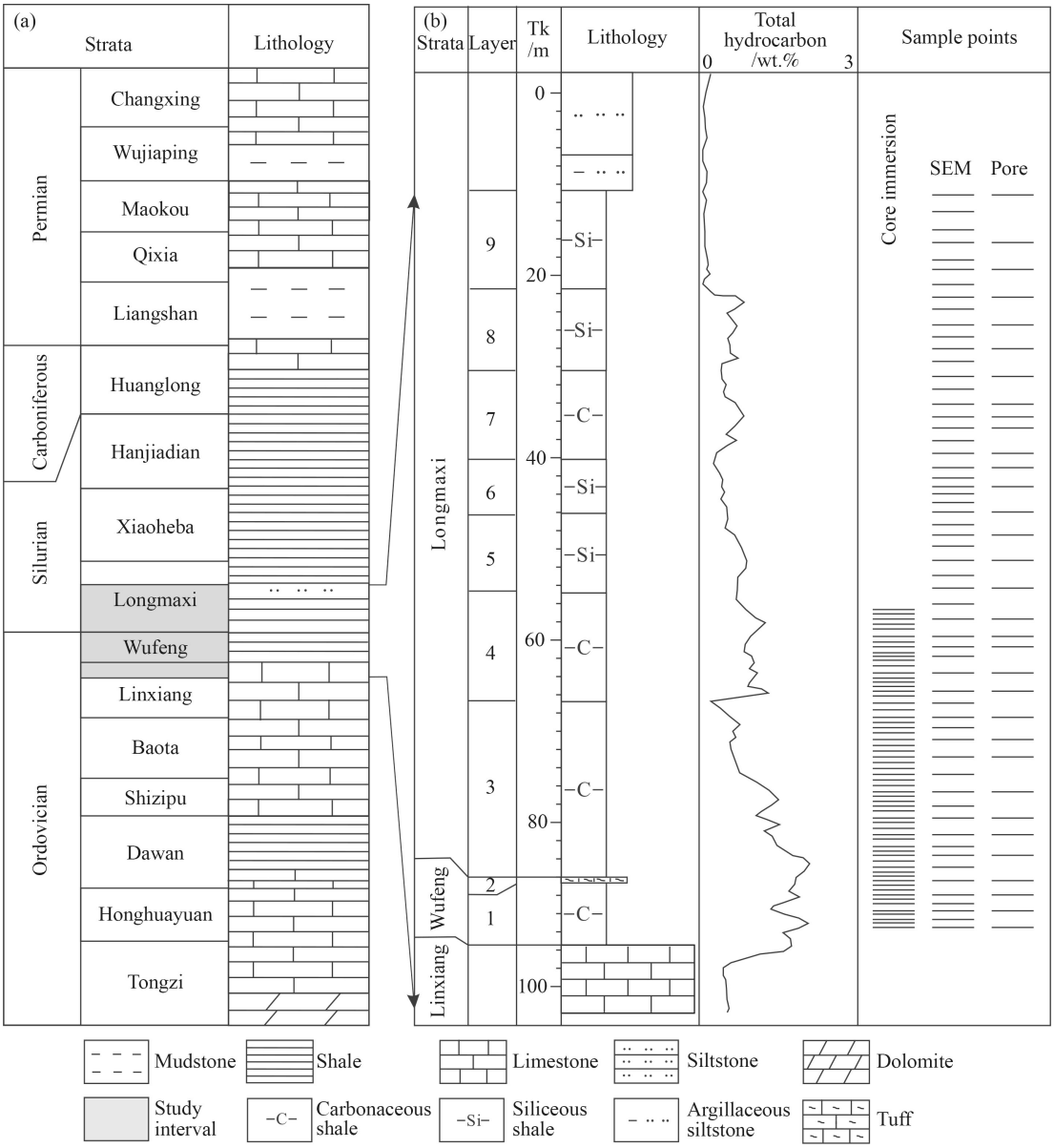

Fig. 2 Stratigraphic sequence and sampling point locations in the study area. (a) Stratigraphic sequence of the Jiaoshiba area; (b) stratification and sampling point locations of the Wufeng and Longmaxi Formations; TK: Thickness.

vary from 5 m to 40 m. During the period of Wufeng Formation deposition, the water body was deeper, and it was also a high-quality shale gas reservoir section. The sedimentary thickness in the target area was 6 m, which was previously the center of sedimentation. Based on core and geochemical trace element analyses, Zhao et al. (2023) demonstrated that the sedimentation period of the high-quality reservoir section of the Wufeng and Longmaxi Formations corresponded to an oxygen-deficient or hypoxic environment rich in organic matter. In the upper section of the Longmaxi Formation, the sedimentary environment changed, causing damage to the organic matter.

2.2 Experimental methods

2.2.1 Immersion test

Water was injected into a transparent glass box with dimensions of 40 cm × 30 cm × 20 cm until the water reached 1/2 the height of the glass box. A total of 2−4 broken cores per meter with lengths of no more than 30 cm were selected. All the cores were immersed in water for at least 10 s, and bubbles were observed emerging from the cores (Fig. 3). After the bubbles stabilized, the location and frequency of all the bubble points on the core were counted every 5 cm.

2.2.2 Wet illumination method for bedding fracture statistics

In dry rock cores, the naked eye cannot easily recognize bedding fractures, and only after the core is wet and immediately prior to air drying can some fracture characteristics be observed (Figs. 4(a) and 4(b)). At present, wet observation of rock cores and statistical analysis of shale bedding fractures are commonly used methods (Guo et al., 2017). When the filling material, such as calcite veins, completely fills the fracture area and the rock core is immediately prior to air drying after wetting, water infiltration into the core can also be observed, indicating that there should also be a small fracture space between the filling joint and the rock mass (Fig. 4(c)).

2.2.3 Logging bedding fracture statistics

Based on the accuracy of various logging interpretation methods, the microresistivity imaging method (FMI) in imaging logging was selected for fracture identification-related work. This ensures that fractures greater than 0.5 mm can be fully identified, and the correlation between conventional logging methods and fractures interpreted from imaging logging can be studied. To clarify the relationship between imaging data and actual

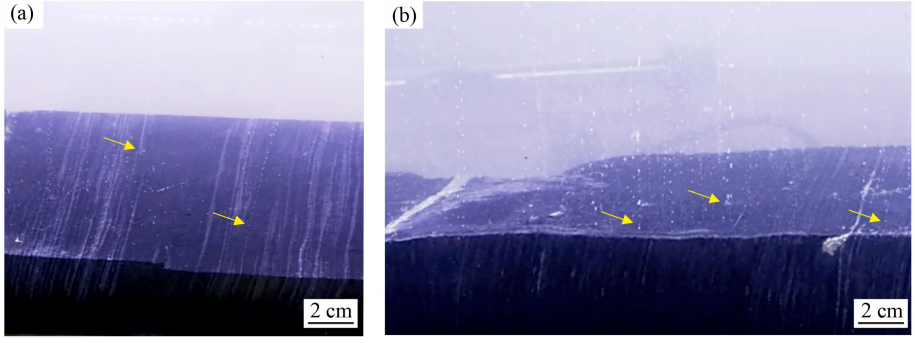

Fig. 3 Core immersion and bubbling experiment. (a) Well A2, 2331.56 m, gray black carbonaceous mudstone; (b) Well A2, 2334.35 m, interbedded with gray black carbonaceous shale and gray argillaceous siltstone.

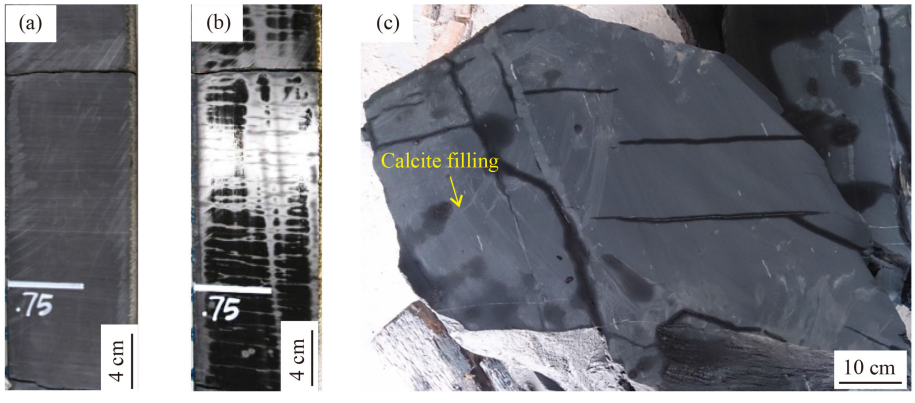

Fig. 4 Characteristics of bedding fractures and fracture filling on the surface of shale. (a) Dry core, with no fractures found on the surface of the shale; (b) wet core with clear fractures; (c) wet calcite-filled fractures, with obvious water absorption in fractures.

geological conditions, depth matching between the images and core was performed. The Wufeng Formation shale and the underlying Jiancaogou Formation limestone are obvious boundary and marker layers in the study area. The corresponding relationships between the core and imaging data can be determined by overlapping the common logging interface, features in core photographs, and imaging logging features (Fig. 5).

2.2.4 Physical property analysis

The effective porosity generally refers to the proportion of the interconnected pore volume to the total volume under corresponding experimental conditions, excluding isolated pores. The effective porosity was measured using an ULTRA-Poro300 porosity measuring instrument, with pore volume measurements ranging from 0.02 to 25 cm^3. High-purity helium gas with a purity of 99.99% was used as the main measurement medium. The basic principle of this method is to measure and calculate the volume of dry rock particles based on Boyle's law; then, the porosity of the rock core can be calculated. First, we sampled a cylindrical plug with a diameter of 2.5 cm and a height of 2–3 cm and cleaned the samples with solvents such as *n*-hexane, acetone, and dichloromethane. After the rock samples were cleaned, they were placed in a drying oven at a temperature of 56°C and baked to a constant weight. A Vernier caliper was used to measure the length and diameter of the plunger sample and calculate the total volume V_t. A helium gas medium was used to measure the particle volume (V_s) of the dried rock core and to calculate the porosity. The porosity of the rock core can be calculated according to the following equation:

$$\Phi = (V_t - V_s)/V_t \times 100\%, \quad (1)$$

where Φ is the porosity, %; V_t is the total volume of the core sample, cm^3; and V_s is the particle volume of the sample, cm^3.

The permeability range of shale reservoirs is usually 10^{-3}–10^{-6} mD, and permeability is also a key reference indicator for estimating the shale oil production capacity. Currently, in the laboratory, pulse attenuation permeability measurement technology based on nonstationary seepage technology is used. The NDP-605 pulse ultralow permeability instrument uses the pulse attenuation method to automatically measure the permeability of shale cores under simulated reservoir pressure and constant temperature conditions. The permeability measurement range is 1×10^{-5}–0.5 mD, and the pore pressure is adjusted using an accurate gas regulator, with a maximum pressure of 17 MPa and a maximum overburden pressure of 70 MPa. High purity nitrogen gas is used as the working medium. The measurement and control system of the instrument first provides pore pressure to the core and then transmits a pressure difference pulse through the core, accompanied by the instantaneous conduction of pressure through the entire core. The computer measurement system records the pressure difference at both ends of the core, downstream pressure and duration and plots the logarithmic curves of the pressure difference and downstream pressure and duration. Thus, linear regression calculations of permeability were performed for various values, such as the pressure difference and duration.

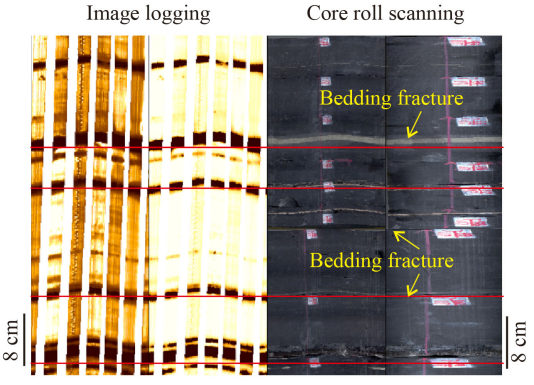

Fig. 5 Schematic diagram of the imaging log and bedding fracture data.

3 Results

3.1 Quantitative characteristics of bedding fractures observed in rock cores

The wet core method (naked eye identification) reveals that the density of fractures in the Wufeng–Longmaxi shale in Well A2 gradually decreases from bottom to top, with a maximum of 437 m and a minimum of 52 m. The bottom 1–3 layers have the most fractures, with an average of 257.6 fractures per meter, and the top 7–8 layers have an average of 176.8 fractures per meter, with relatively few other layers (Fig. 6(a)). Moreover, the number of bedding layers in 1–5 small layers of shale was also counted, and there is a strong positive correlation between the number of bedding layers and the number of bedding fractures. In the part with the greatest development of bedding fractures, the bedding layers are also the most developed, corresponding to 1597 pieces/m, and 127 pieces/m in the part with the least development of bedding fractures (Fig. 6(b)).

The immersion experiment revealed that when the shale core (without filling material or upper rock filling) is vertically emplaced, no gas outlet points are present on the top surface of the core, and there are gas outlet points on the side. The speed of natural gas release is moderate, and the bubbles are generally small and short in duration. In addition, when there is a calcite vein on the top surface, there are abundant gas release points on the surface of the calcite vein, with large bubbles. The gas release speed is fast with long duration.

When the rock core is emplaced horizontally (filled

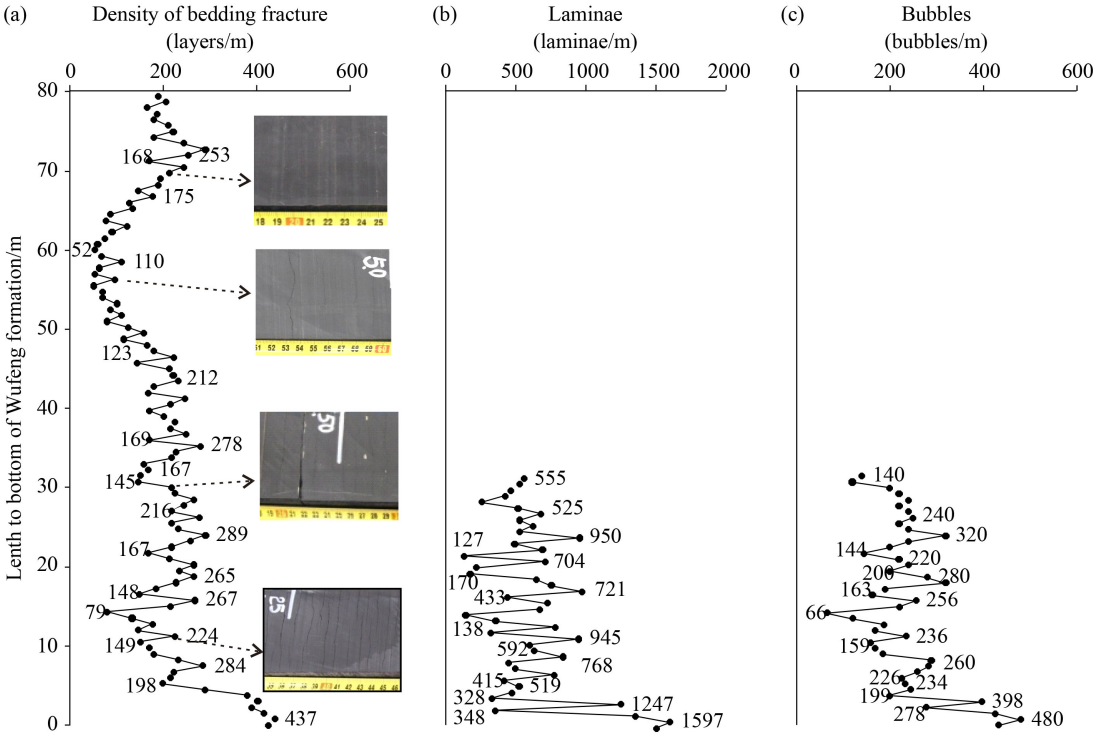

Fig. 6 Quantitative characteristics of bedding, bedding fractures, and number of bubbles in Well A2.

with calcite), there are many bubbling points on the side of the unfilled rock core, and the gas stored in the shale migrates outward from these bubbling points. Some layers have more bubbles, while others have fewer bubbles, with a minimum of 36 bubbles per meter and a maximum of 480 bubbles per meter (Fig. 6(c)). Differences in the speed, size, and duration of movement were observed for these bubble points. The bubbling speed ranges from hundreds per second to 2−3 s per bubble. The bubble size ranges from hundreds of microns to a few millimeters, and the bubbling process can last from 2 to 48 h.

3.2 Quantitative characteristics of well logs and bedding fracture interpretations

The interpreted results of the imaging logs reveal that the degree of development of bedding fractures is the highest in sublayer 3, with a maximum of 14 bedding fractures per meter. Sublayer 9 corresponds to the lowest level of bedding fracture development, with a minimum of 0.89 bedding fractures/m. The degree of development of interlayer and foliation fractures in the Wufeng Formation shale reservoir is not high, with an average of 7.47 bedding fractures per meter. The extent of nonstructural fracture generation in the Longmaxi Formation shale reservoir gradually decreases from bottom to top (Fig. 7).

3.3 Physical properties of bedding fractures

Sampling in the vertical bedding direction is more

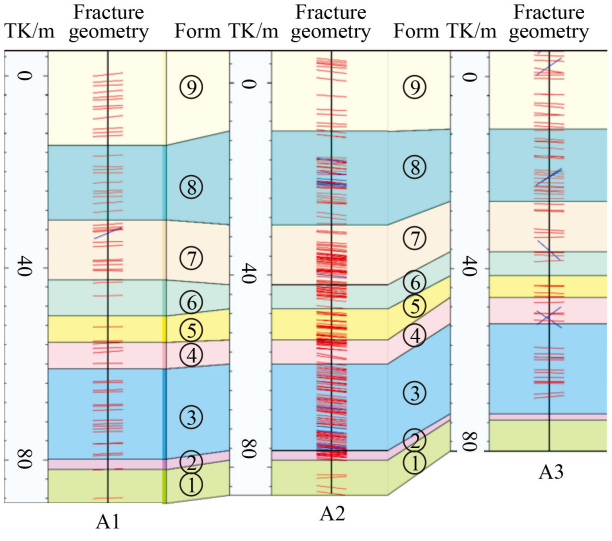

Fig. 7 Quantitative characteristics of bedding fractures in the Wufeng–Longmaxi Formations based on imaging logging; TK: Thickness.

difficult than in the parallel bedding direction. Thus, 155 samples in the parallel bedding direction were obtained, including 21 samples from Well A1, 65 samples from Well A2, and 69 samples from Well A3 (Fig. 8(a)). There were 56 samples in the vertical direction, including 15 samples from Well A1, 8 samples from Well A2, and 33 samples from Well A3 (Fig. 8(b)).

The samples taken in the vertical bedding direction have porosities ranging from 0.3% to 7.1% and an average porosity of 3.1%. The minimum permeability is 0.01 mD, the maximum permeability is 13.43 mD, and

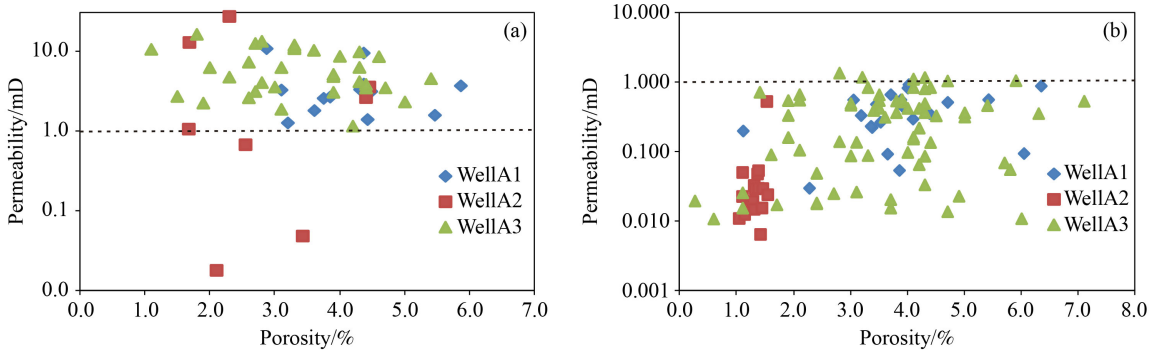

Fig. 8 Comparison of the matrix and fracture permeabilities of the marine shale reservoir in the Longmaxi Formation. (a) Samples taken in the parallel bedding direction; (b) samples taken in the vertical bedding direction.

the average permeability is 0.62 mD. Most samples have permeability values less than 1 mD. The minimum porosity of the samples in the parallel bedding direction is 1.1%, the maximum porosity is 7.1%, and the average porosity is 3.6%. The minimum permeability is 0.02 mD, the maximum is 27.63 mD, and the average permeability is 5.6 mD. Most samples have permeabilities greater than 1 mD. The average porosity of the vertically bedded shale samples is basically the same as that of the parallel-bedded shale samples. The average permeability of parallel-bedded shale samples is 44.6 times that of vertically bedded shale samples, indicating that bedding fractures have a significant impact on shale reservoir permeability (Fig. 8).

4 Discussion

4.1 Filling properties of bedding fractures

The core observation results of three existing wells in the work area suggest that filled fractures account for 67% of the total number of fractures and that unfilled fractures account for 33% of the total structural fractures. The filling materials include calcite, pyrite, mud, and their mixture. Under high-resolution electron microscopy, a large number of internally connected intergranular pores can be observed in pyrite, which constitute effective flow space (He et al., 2017b; Wang et al., 2019a, 2019b; Wang et al., 2022b; Zhu et al., 2022). Therefore, fractures filled by pyrite can be regarded as gas-flow-effective fractures. Moreover, on-site experiments have suggested that fractures filled with calcite are also effective channels for shale gas migration. Based on a comparison experiment between fractures filled with calcite and unfilled fractures, Wang et al. (2018a) found that filling fractures filled with calcite did affect the seepage of shale gas.

Calcite veins are formed by the later crystallization of calcite dissolved in fluids and are closely related to dissolution (Urai et al., 1991). The temperatures of the calcite inclusions in the shale fractures of the Wufeng Formation in the Jiaoshiba area range from 196.2°C to 239.5°C, indicating that calcite veins formed in the early Late Cretaceous when the strata exhibited the maximum burial depth throughout their history. In the early Late Cretaceous, a good spatiotemporal matching relationship with the completion of dissolution was exhibited (Wang et al., 2022a). The fractures filled with calcite veins are channels for the flow of shale gas. According to on-site immersion experiments, these calcites are confirmed to be connected. No bubbles appear on the cross-section of the shale, except for the part filled with calcite, which emitted bubbles. Moreover, compared to shale reservoirs that are not filled with calcite, the strength and speed of bubbling are greater. The calcite veins connect with the pores inside the shale reservoir and are good channels for shale gas. The pore spaces inside calcite are also connected. The characteristics of calcite vein distribution also indirectly indicate the connectivity of shale reservoirs (Fig. 9).

4.2 Opening of bedding fractures

Regional structural fractures generally play a destructive role in shale gas development, and it can be inferred that most of these fractures are in an open state, connecting reservoirs to nonreservoirs and leaking shale gas (Wang et al., 2016, 2018b, 2021; Liu et al., 2018). There is currently significant controversy over whether shale reservoir fractures, especially interlayer and lamination fractures, are open. Most scholars believe that open fractures above ground should be in a closed state underground. Imaging logging calibration interpretation, core immersion experiments, and overburden pressure experiments suggest that underground underlying fractures should be in an open state, but the number of fractures is relatively low (Wang et al., 2018a; Fu et al., 2022; Liu et al., 2022; Yao et al., 2022).

Through immersion experiments and MAPS microscopy image features, it was found that in the areas where fractures cannot be identified with the naked eye, there are gas outlets in the core, which are small-scale foliation fractures (Wang et al., 2018a). The bedding fractures are open underground (Wang et al., 2019b). A comparison

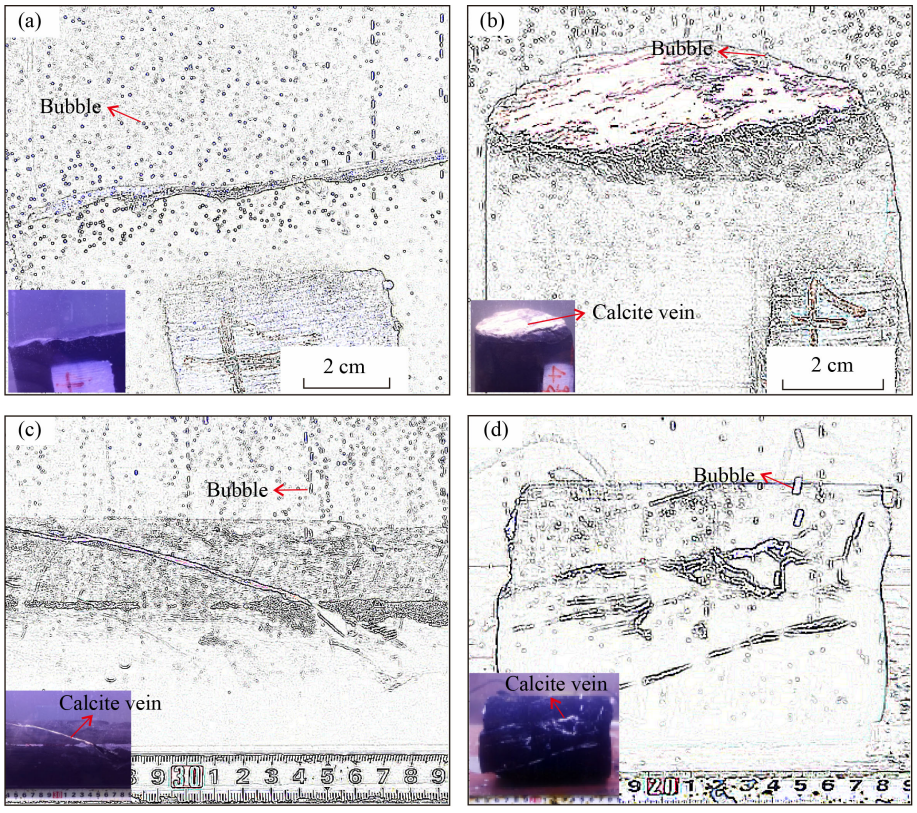

Fig. 9 Bubble characteristics of the calcite vein during the immersion experiment. (a) At a distance of 18.6 m from the bottom of the Wufeng Formation, gray black carbonaceous shale formed. When the rock core is horizontally emplaced, there is a large amount of bubbling in a point-like manner, and most of the bubbling points appear at a certain point between the bedding planes. (b) At a distance of 12.3 m from the bottom of the Wufeng Formation, gray black carbonaceous shale is observed. When the core is vertically emplaced, a large number of bubbling points are observed on the detachment surface of the top surface of the core. (c) At a distance of 4.2 m from the bottom of the Wufeng Formation, black carbonaceous shale with fractures partially filled with calcite, and the bubbles at the fractures are more intense. (d) At a distance of 4.2 m from the bottom of the Wufeng Formation, black carbonaceous shale with fractures fully filled with calcite, and there is intense bubbling at the fractures.

and calibration of the shale bands and low-angle fractures in the core with the imaging log data reveal that the filled fractures exhibit good response characteristics according to the imaging log data. Moreover, the layers that cannot be determined on the rock core also exhibit good response characteristics in terms of imaging logging, indicating that the rock core that fractured above ground also fractured underground. Moreover, the imaging logging and core comparison maps reveal that when the size of the fractures is small or when there is no response shown in imaging logging, more precise methods are needed to identify smaller foliation fractures. However, it is evident that smaller levels of open-state bedding fractures do exist (Fig. 10).

4.3 Influence of bedding fractures on physical properties

The fracture network system in shale reservoirs is composed of bedding fractures, cohesive fractures, and dissolution fractures (Wang et al., 2019a). The existence of bedding fractures greatly increases the permeability of shale reservoirs in parallel bedding directions, and the magnitude of permeability is positively correlated with the degree of bedding fracture opening. The stress sensitivity of fracture-type pores is extremely strong. Compared to that of matrix pores, the porosity of fracture type pores mainly composed of bedding fractures decreases to approximately 40% under a 30 MPa confining pressure. The stress sensitivity of the matrix pores is much weaker than that of the crack-type pores; however, the matrix porosity generally remains above 85% of the initial value under confining pressures of 30−50 MPa. Based on normal temperature and pressure experiments, most scholars believe that fractures are closed under geological conditions, while others believe that fractures will open during the process of reservoir structural uplift (He et al., 2017b). To understand the true state of microfractures in underground reservoirs, overburden pressure experimental research and practical operation were also conducted. Previously, the effective stress was measured only at 25 MPa, and the drilling depth has developed toward deeper layers. To better apply and guide the direction of future exploration and development, this study increased the pressure to 40 MPa.

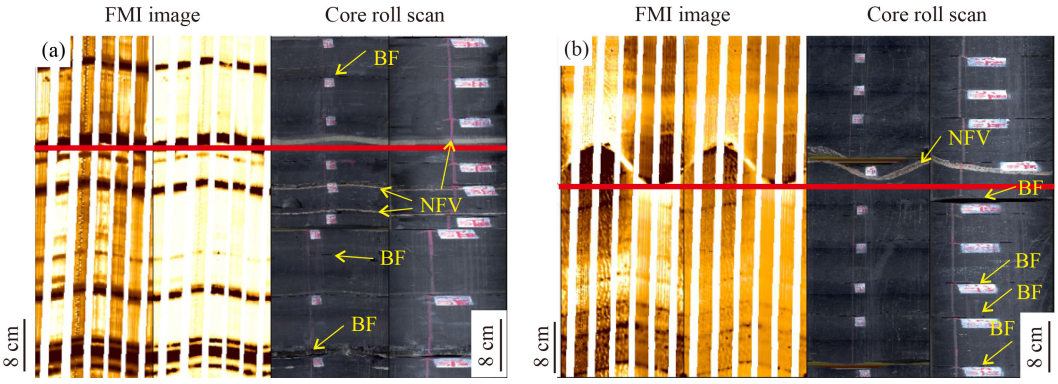

Fig. 10 Response characteristics of bedding fracture imaging logs. (a) Well A2 2463.52-2464.35; (b) Well A2 2468.43-2469.17; BF: Bedding fracture, NFV: Vein-filling fracture.

The experimental results indicate that as pressure increases, the permeability of shale reservoirs gradually decreases (Fig. 11(a)). When the effective stress increases to more than 35 MPa, the compression ratio of microfractures approaches 0%, indicating that the microfractures are in a closed state. According to this effective stress calculation, when the burial depth of the shale reservoir reaches approximately 3500 m and assuming that the pore fluid pressure is 0 MPa, the underground reservoir microfractures are in a closed state. The Jiaoshiba shale reservoir is in an overpressured state, and it can be inferred that the microfractures in the shale reservoir are in an open state.

After hydraulic fracturing, a fracturing transformation area is formed (Figs. 11(b)–11(d)), and the presence of a natural fracture network can provide continuous channels for later production of shale gas. The Fuling Shale Gas Field has transitioned from the second-generation fracturing technology of "multicluster dense cutting+ball throwing+continuous sand addition" to the third-generation fracturing technology of "multisegment multicluster dense cutting+flow-limiting fracturing+high-strength sand addition," which has significantly increased the production of single-well tests and greatly reduced fracturing costs. Moreover, in response to the difficulties of increasing the absolute value of *in situ* stress in deep shale and the high degree of closure of bedding fractures and microfractures, the technology of subdividing sections and increasing diversion has been adopted to achieve effective development of deep shale gas in the Fuling Jiangdong Block. Thus, bedding fractures play more critical roles in the efficient application of hydraulic fracturing and should be considered in the design and evaluation periods.

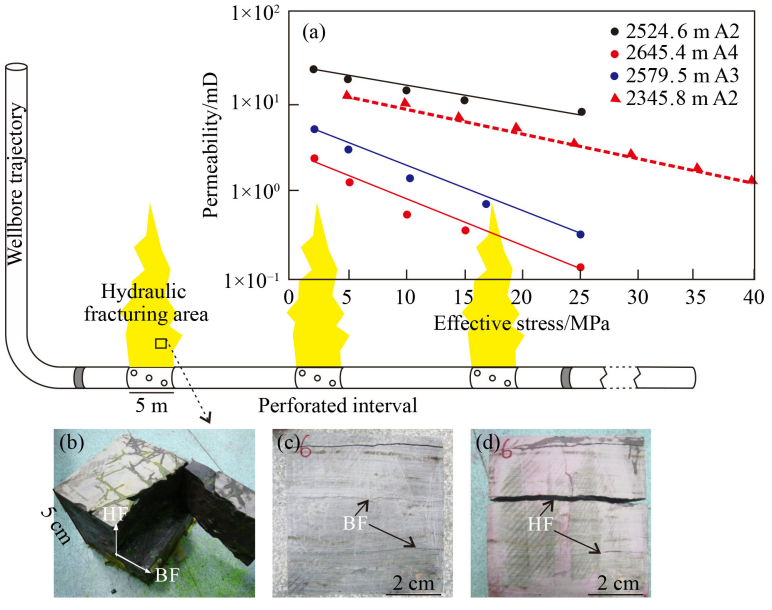

Fig. 11 Impact of bedding fractures on physical properties in the original formation and fracture reconstruction area. (a) Relationship between the magnitude of effective stress and permeability changes. The sample was taken from Well A2. (b) Experimental results of hydraulic fracturing of layered shale. (c) The state of bedding fractures before fracturing. (d) The state of bedding fractures after fracturing. BF: Bedding fracture, HF: Hydraulic fracture.

5 Conclusions

Bedding fractures are highly developed in shale reservoirs, with a minimum density of 36/m and a maximum density of 480/m. Filled and unfilled fractures account for 67% and 33%, respectively, of the total number of fractures.

Bedding fractures have a weak effect on porosity and can increase permeability by two orders of magnitude. The average porosity difference between the vertically bedded and parallel-bedded shale samples is inconspicuous, while the average permeability of the parallel-bedded shale samples is 44.6 times that of the vertically bedded shale samples.

Bedding fractures open underground. The drill core bedding fractures are strongly correlated with the response characteristics observed by imaging logging, and the opening of bedding fractures can be calculated from imaging logging data. The porosity and permeability of calcite-filled fractures affect the seepage of shale gas.

Bedding fractures are efficient seepage channels for shale reservoirs. The utilization and transformation of bedding fractures during the fracturing process are the keys to shale oil and gas reservoir development. By integrating the *in situ* stress field, bedding fracture development, and shale compressibility, the reasonable use of bedding fractures is valuable when analyzing oil and gas reservoirs.

Acknowledgments This research was sponsored by the China Postdoctoral Science Foundation (No. 2021M703000): Formation mechanism of a compressive fracture network constrained by weak surfaces of shale bedding. We thank the Sinopec Exploration Company and the Sinopec Jianghan Oilfield for their valuable data and information.

Competing interests The authors declare that they have no competing interests.

References

BP (2022). Statistical review of world energy. Available at BP website

Dai J, Ni Y, Liu Q, Wu X, Gong D, Hong F, Zhang Y, Liao F, Yan Z, Li H (2021). Sichuan super gas basin in southwest China. Pet Explor Dev, 48(6): 1251–1259

EIA(2018). Energy Information Administration. Short-Term Energy Outlook

Fu X, Gong L, Su X, Liu B, Gao S, Yang J, Qin X (2022). Characteristics and controlling factors of natural fractures in continental tight-oil shale reservoir. Minerals (Basel), 12(12): 1616

Gale J F, Laubach S E, Olson J E, Eichhubl P, Fall A (2014). Natural fractures in shale: a review and new observations. AAPG Bull, 98(11): 2165–2216

Guo X, Hu D, Li Y, Wang Z, Wang X, Liu Z (2017). Geological factors controlling shale gas enrichment and high production in Fuling shale gas field. Pet Explor Dev, 44(4): 513–523

He D, Lu R, Huang H, Wang X, Jiang H, Zhang W (2019). Tectonic and geological setting of the earthquake hazards in the Changning shale gas development zone, Sichuan Basin, SW China. Pet Explor Dev, 46(5): 1051–1064

He Z, Hu Z, Nie H, Li S, Xu J (2017a). Characterization of shale gas enrichment in the Wufeng Formation–Longmaxi Formation in the Sichuan Basin of China and evaluation of its geological construction–transformation evolution sequence. J Nat Gas Geosci, 2(1): 1–10

He Z, Nie H, Zhao J, Liu W, Bao F, Zhang W (2017b). Types and origin of nanoscale pores and fractures in Wufeng and Longmaxi shale in Sichuan Basin and its periphery. J Nanosci Nanotechnol, 17(9): 6626–6633

Li Y, Wang S, Zheng L, Zhao S, Zuo J (2021). Evaluation of the fracture mechanisms and criteria of bedding shale based on three-point bending experiment. Eng Fract Mech, 255: 107913

Liu D, Ge H, Shen Y, Liu H, Zhang Y (2021). Experimental investigation on imbibition characteristics of shale with highly developed bedding fractures. J Nat Gas Sci Eng, 96: 104244

Liu J, Ding W, Dai S, Gu Y, Yang M, Sun B (2018). Quantitative multiparameter prediction of fault-related fractures: a case study of the second member of the Funing Formation in the Jinhu Sag, Subei Basin. Petrol Sci, 15(3): 468–483

Liu Y, Yang H, Zhang Q, Xiong D (2022). Properties of a shale bedding plane and its influence on the geometric parameters of fracture propagation in volume fracturing. Eng Fract Mech, 266: 108413

Nie H, He Z, Liu G, Du W, Wang R, Zhang G (2021). Genetic mechanism of high-quality shale gas reservoirs in the Wufeng–LongmaxiFms in the Sichuan Basin. Natural Gas Industry B, 8(1): 24–34

OPEC (2018). World Oil Outlook. Available at OPEC website

Solarin S A, Gil-Alana L A, Lafuente C (2020). An investigation of long range reliance on shale oil and shale gas production in the US market. Energy, 195(2020): 116933

Sun J, Bao H (2018). Comprehensive characterization of shale gas reservoirs: a case study from Fuling shale gas field. Petroleum Geology & Experiment, 40(1): 1–12 (in Chinese)

Urai J L, Williams P F, Van Roermund H L M (1991). Kinematics of crystal growth in syntectonic fibrous veins. J Struct Geol, 13(7): 823–836

Wang H, He Z, Jiang S, Zhang Y, Nie H, Bao H, Li Y (2022a). Genesis of bedding fractures in Ordovician to Silurian marine shale in Sichuan Basin. Energies, 15(20): 7738

Wang H, He Z, Zhang Y, Bao H, Su K, Shu Z, Zhao C, Wang R, Wang T (2019a). Dissolution of marine shales and its influence on reservoir properties in the Jiaoshiba area, Sichuan Basin, China. Mar Pet Geol, 102: 292–304

Wang H, He Z, Zhang Y, Su K, Wang R (2018a). Quantitative identification of microfractures in the marine shale reservoir of the Wufeng-Longmaxi Formation using water immersion tests and image characterization. Interpretation (Tulsa), 6(4): SN23–SN30

Wang H, He Z, Zhang Y, Su K, Wang R, Zhao C (2019b). Microfracture types of marine shale reservoir of Sichuan Basin and its influence on reservoir property. Oil Gas Geol, 40(1): 41–49

Wang R, Ding W, Zhang Y, Wang Z, Wang X, He J, Zeng W, Dai P

(2016). Analysis of developmental characteristics and dominant factors of fractures in Lower Cambrian marine shale reservoirs: a case study of Niutitang Formation in Cen'gong block, southern China. J Petrol Sci Eng, 138: 31–49

Wang R, Hu Z, Liu J, Wang X, Gong D, Yang T (2018b). Comparative analysis of characteristics and controlling factors of fractures in marine and continental shales: a case study of the Lower Cambrian in Cengong area, northern Guizhou Province. Oil Gas Geol, 39(4): 631–640

Wang R, Hu Z, Long S, Du W, Wu J, Wu Z, Nie H, Wang P, Sun C, Zhao J (2022b). Reservoir characteristics and evolution mechanisms of the Upper Ordovician Wufeng-Lower Silurian Longmaxi shale, Sichuan Basin. Oil Gas Geol, 43(2): 353–364

Wang R, Hu Z, Long S, Liu G, Zhao J, Dong L, Du W, Wang P, Yin S (2019c). Differential characteristics of the Upper Ordovician-Lower Silurian Wufeng-Longmaxi shale reservoir and its implications for exploration and development of shale gas in/around the Sichuan Basin. Acta Geol Sin (English Ed), 93(3): 520–535

Wang R, Hu Z, Zhou T, Bao H, Wu J, Du W, He J, Wang P, Chen Q (2021). Characteristics of fractures and their significance for reservoirs in Wufeng-Longmaxi shale, Sichuan Basin and its periphery. Oil Gas Geol, 42: 1295–1306

Yao C, Fu H, Ma Y, Yan D, Wang H, Li Y, Wang J (2022). Development characteristics of deep shale fractured veins and vein forming fluid activities in Luzhou Block. Earth Sci, 47(5): 1684–1693

Zhao L, Mao W, Liu Z, Cheng S (2023). Research on the differential tectonic-thermal evolution of Longmaxi shale in the southern Sichuan Basin. Adv Geo-Energy Res, 7(3): 152–163

Zhou S, Jiang W, Zhang C, Fan B (2012). The enlightenment on shale gas exploration and development in China getting from Eagle Ford in America. Eng Sci, 14(6): 16–21

Zhu H, Chen L, Cao Z, Wang M, Hong H, Li Y, Zhang R, Zhang S, Zhu G, Zeng X, Yang W (2022). Microscopic pore characteristics and controlling factors of black shale in the Da'anzhai Member of Jurassic Ziliujing Formation, central Sichuan Basin. Oil Gas Geol, 43(5): 1115–1126

Zou C, Ma F, Pan S, Zhang X, Wu S, Fu G, Wang H, Yang Z (2023). Formation and distribution potential of global shale oil and the developments of continental shale oil theory and technology in China. Earth Sci Front, 30(1): 128–142 (in Chinese)

Zou C, Pan S, Jing Z, Gao J, Yang Z, Wu S, Zhao Q (2020). Shale oil and gas revolution and its impact. Acta Petrol Sin, 41(1): 1–12 (in Chinese)